Composites Part C: Open Access 4 (2021) 100090

Contents lists available at ScienceDirect

Composites Part C: Open Access

journal homepage: www.elsevier.com/locate/jcomc

Flexural behaviour of carbon and glass reinforced hybrid composite pipes

Chensong Dong

School of Civil and Mechanical Engineering, Curtin University, GPO Box U1987, Perth 6845, WA, Australia

ARTICLE INFO

Keywords:
Composite
Pipe
Hybrid
Flexural

ABSTRACT

This paper presents a study on the flexural behaviour of hybrid composite pipes reinforced with carbon and glass fibres. The progressive failure of composite pipes in three point bending was modelled numerically by Finite Element Analysis (FEA). The FEA based model was validated against the experimental data. With this developed model, the effects of ply angle, fibre volume fraction and hybridisation have been found. It is shown from the results that the maximum bending loads occur when the ply angle is between 60° and 75° The hybrid composite pipe has comparable failure loads compared to the full carbon fibre composite pipe or the full glass fibre composite pipe.

1. Introduction

Composite pipes are important structural members in various industries. Research has been done for the failure of composite pipes. Prabhakar et al. [1] presented an overview of burst, buckling, durability and corrosion analysis of lightweight FRP composite pipes and their applicability. Hastie et al. [2] investigated the failure of thermoplastic composite pipes (TCP) under combined pressure, tension and thermal gradient for an offshore riser application. Rafiee [3] reviewed the mechanical performance of glass-fibre-reinforced thermosetting-resin pipes. Most studies on the mechanical performance of composite pipes were focused on internal pressure [4–7], axial loading [6,7], and transverse loading [8]. Very limited have been seen on flexural loading [9–11]. Xia et al. [9] presented an exact solution for thick-walled filament wound composite pipes under pure bending using classical laminated-plate theory. Jonnalagadda et al. [10] presented an analytical model for composite tubes with bend-twist coupling.

Hybrid composite materials have been widely researched in order to take advantage of both virgin composite materials. A common hybrid composite is made by including both carbon and glass fibres in a common polymer matrix. When evaluating the properties of hybrid composites, the deviation from the Rule of Mixtures (RoM) [12] has been noticed by various researchers and is denoted hybrid effect. Positive hybrid effects, i.e. the flexural strength is higher than the RoM, have been notice in the previous research [13–16]. The main reason is that glass fibre has higher strain-to-failure than carbon fibre, the strain-to-failure is increased due to the inclusion of glass fibre [17]. The existence of hybrid effect can be potentially useful for achieving a balanced cost and weight optimal composite material.

It is shown from the literature that most of studies on hybrid composites are for flat specimens and whether hybrid effects exist for hybrid composite pipes is still unclear. This study aims at filling this technical gap. In this study, an approach was developed for modelling the flexural behaviour of hybrid composite pipes in three point bending. The effects of parameters including ply angle, fibre volume fraction and hybridisation were studied.

2. Modelling

2.1. Model development

A composite pipe in three point bending is shown in Fig. 1. The composite pipe is supported by two rollers at a span of L and loaded at its mid-span.

The hybrid composite pipe in three point bending was simulated by FEA using Ansys Workbench. A material model was created for each of the composite materials. Material properties including elastic moduli, Poisson's ratios, shear moduli and strengths were defined. The composite pipe was created as a surface body. The layup including ply materials and ply angles were defined using Ansys ACP. The rollers were created as solid bodies. Frictional contact was defined between the rollers and the composite pipe. A representative finite element mesh is shown in Fig. 2. Two support rollers are fixed and a prescribed displacement 30 mm is applied to the loading roller. Convergence was done and the force-displacement curve was obtained via nonlinear analysis. The stress based failure criteria were applied. When failure occurred in a ply, stiffness degradation factors [18] were used to reduce the stiffness and the progressive failure behaviour was obtained.

E-mail address: c.dong@curtin.edu.au

https://doi.org/10.1016/j.jcomc.2020.100090
Received 4 August 2020; Received in revised form 10 December 2020; Accepted 14 December 2020
2666-6820/© 2020 The Author(s). Published by Elsevier B.V. This is an open access article under the CC BY-NC-ND license (http://creativecommons.org/licenses/by-nc-nd/4.0/)

Table 1
Pipe designs for validation.

Pipe design	Winding design (outside to inside)	Inside diameter (mm)	Thickness (mm)
1	$[60_5/90_2]$	100	6
2	$[60_{11}/90_2]$	100	10.5
3	$[60_2/30_4/90_2/10_3/90_2]$	100	10.5
4	$[60/30_4/90/10_2/90/10_2/90_2]$	100	10.5

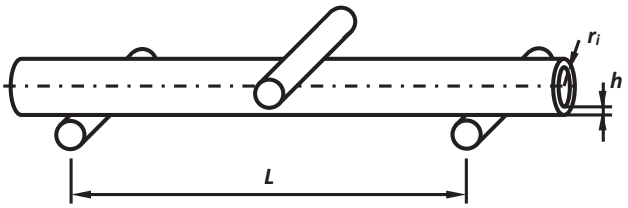

Fig. 1. A composite pipe in three point bending.

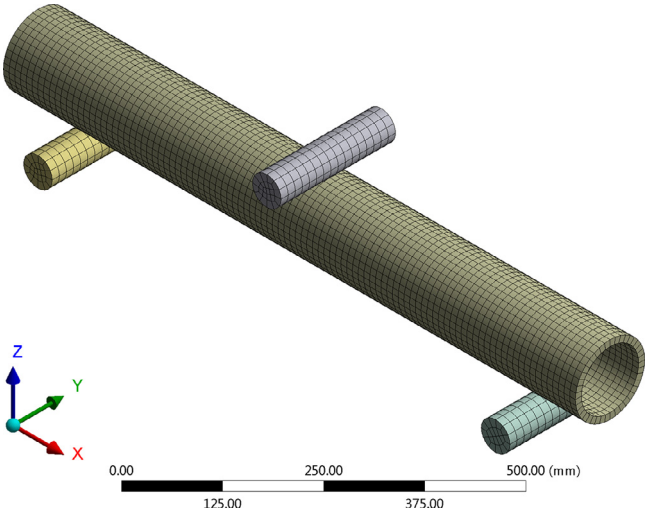

Fig. 2. FEA model of composite pipe.

2.2. Model validation

The developed FEA based model was validated against the experimental data in [11]. Four winding designs were simulated, as shown in Table 1. Each winding design contains a number of plies of various winding angles. The axial direction of the pipe is 0° and the hoop direction is 90° For each winding design in Table 1, the layup from left to right corresponds to the plies from outside to inside. Thus, the innermost ply is 90° and the outermost ply is 60° A prescribed displacement of 30 mm was applied to the loading nose.

For pipe design 4, the deformation from FEA is shown in Fig. 3. The axial stresses of the outermost ply (ply 1) and the innermost ply (ply 13) at the maximum displacement are shown in Fig. 4. The maximum failure criteria of the outermost ply (ply 1) and the innermost ply (ply 13) are shown in Fig. 5. It is shown from Figs. 4 and 5 that the maximum stress and failure occur at the mid-span of the pipe.

It should be noted that progressive failure occurs at this displacement. The first ply failure occurs when the displacement is around 6.15 mm, and the distribution of axial and hoop stresses throughout all plies are shown in Fig. 6. It is shown that the stresses on the compressive side are much higher compared to those on the tensile side, which is in agreement with failure initiating on the compressive side.

The load-displacement curves from the experiment and FEA predictions are shown in Fig. 7. Two different degradation factors 0.9 and 0.99 were chosen in the FEA. It is shown that the experimental failure load is close to the FEA prediction when the degradation factor is 0.99, i.e. total degradation.

When the stiffness degradation factor is 0.9, the experimental, theoretical and FEA failure loads are shown in Fig. 8. It is shown that the FEA predictions agree with the theoretical results but are higher than the experimental results. The actual failure load falls in a range when a degradation factor between 0.9 and 0.99 is applied.

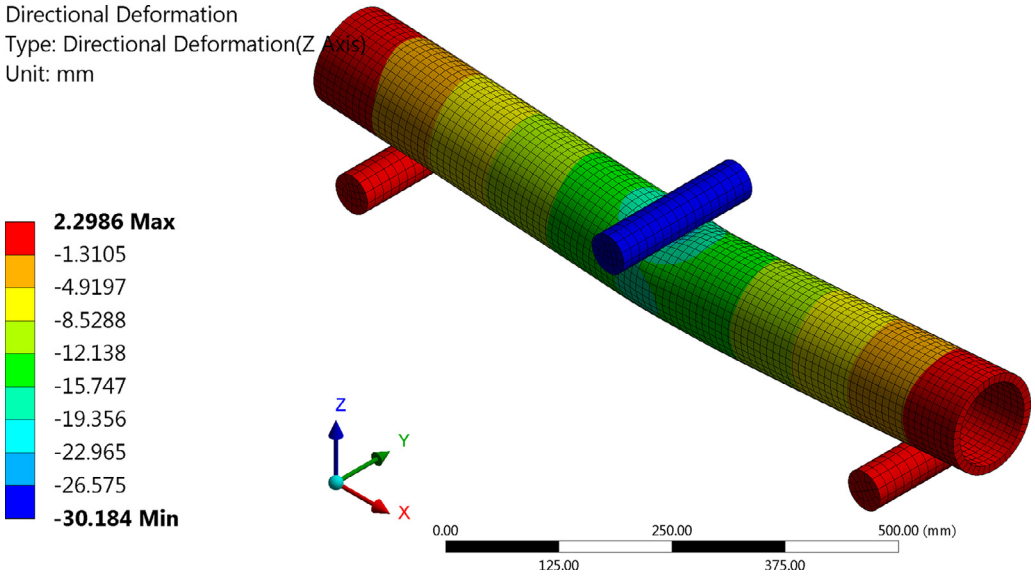

Fig. 3. Deformation of composite pipe.

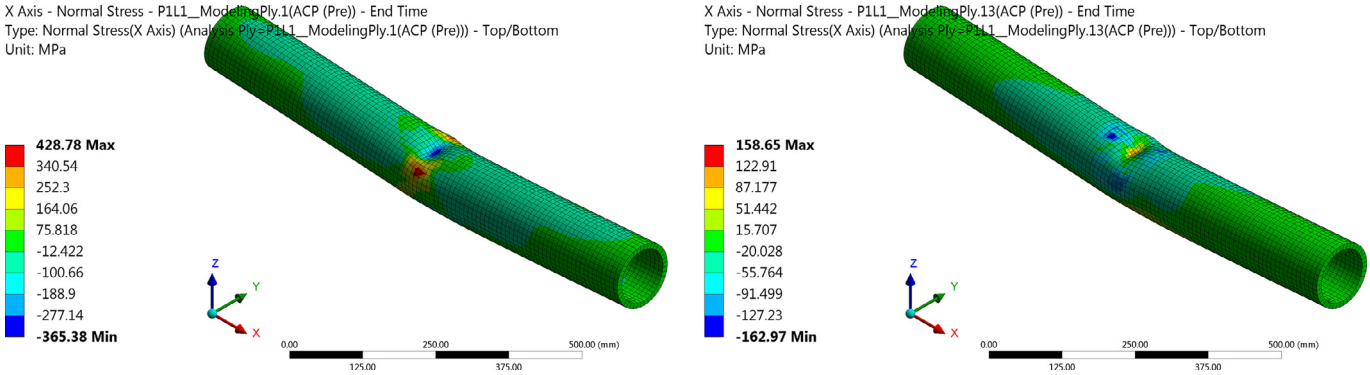

Fig. 4. Stresses from FEA; Left: outermost layer; right: innermost layer.

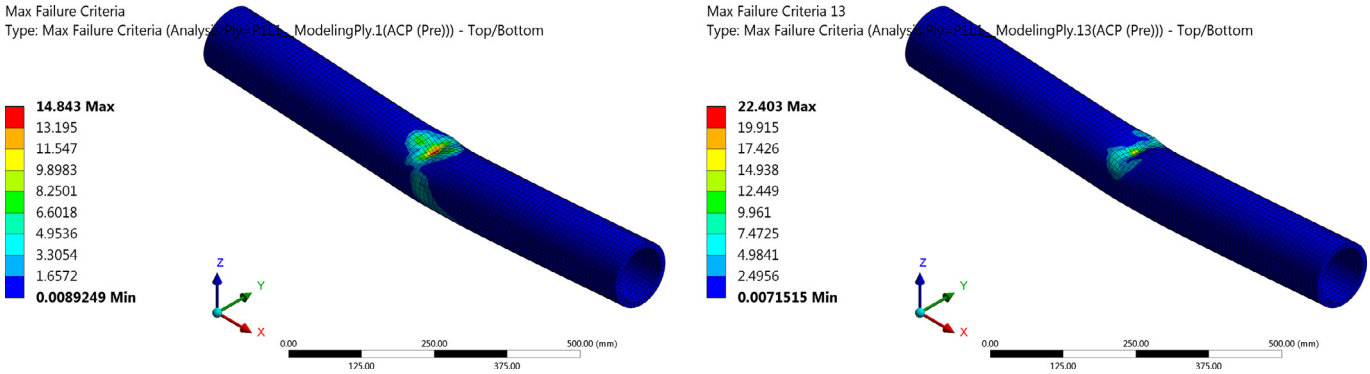

Fig. 5. Maximum failure criteria from FEA; Left: outer layer; right: inner layer.

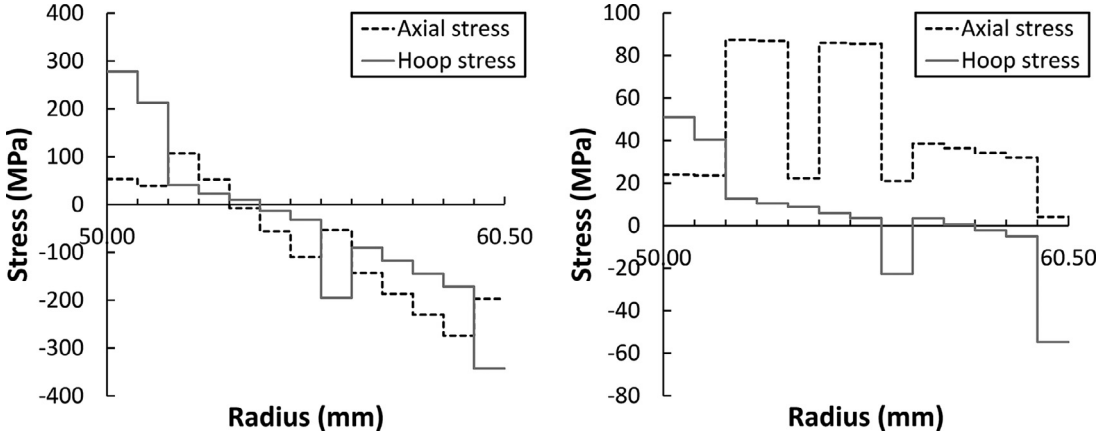

Fig. 6. Stress distribution throughout all plies: Left: compressive side; right: tensile side.

2.3. Model application

The fibres being used in this study include T700S carbon and S-2 glass fibres. The matrix employed in the procedure is Kinetix® R240 high performance epoxy resin combined with Kinetix® H160 hardener (ATL Composites, Southport Queensland 4215, Australia) with a recommended mixing ratio of 100:25. Epoxy resins are widely used in composites because of their high strength (tensile, compressive and flexural), good chemical resistance, fatigue resistance, corrosion resistance and electrical resistance [19]. The properties of the fibres and epoxy resin are presented in Table 2 [13].

For each lamina, based on the constituent properties and its fibre volume fraction, the lamina properties, including the longitudinal modulus E_{11}, the transverse moduli E_{22} and E_{33}, and the shear moduli G_{12}, G_{13} and G_{23}, are derived by Hashin's model [20]. The strength components of composites were derived and stress based failure criteria were employed. For the purpose of modelling the progressive failure, the stiffness degradation factor was chosen to be 0.9.

The hybrid composite pipe in this study consists of eight laminas and the thickness of each lamina is 0.25 mm. The pipe length is 1000 mm. The inner radius is 50 mm. The span is 832 mm. Various pipe designs were investigated by the FEA based model, with the purpose of understanding the effects of ply angle, fibre volume fraction and hybridisation.

3. Results and discussion

3.1. Effect of ply angle

The fibre volume fractions of the carbon/epoxy and glass/epoxy plies were chosen to be 30% and 50%, respectively. The stacking sequence

Table 2
Selected properties of fibres and resin.

Material	Tensile strength (MPa)	Tensile modulus (GPa)	Density (g/cm^3)
S-2 glass unidirectional Unitex plain weave UT-S500 fibre mat (SP System, Newport, Isle of Wight, UK)	4890	86.9	2.46
Toray T700S 12 K carbon fibre (Toray Industries Inc, Tokyo, Japan)	4900	230	1.8
Kinetix R240 high performance epoxy resin with H160 hardener at a ratio of 4:1 by weight, as recommended by manufacturer (ATL Composites Pty Ltd, Australia)	69.6	3.1	1.09

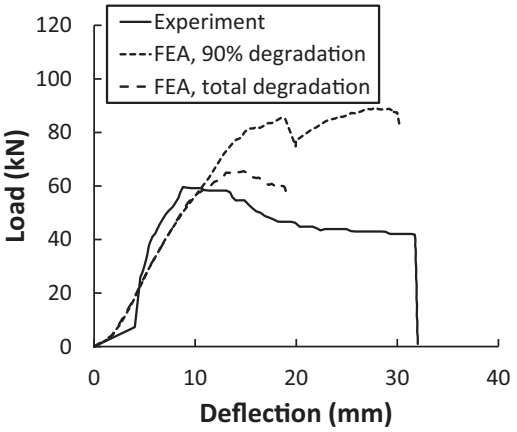

Fig. 7. Load-displacement curves.

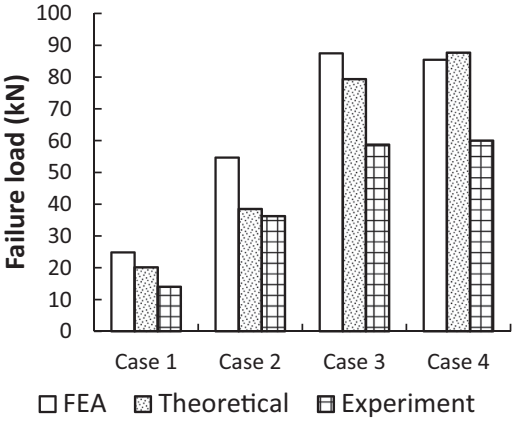

Fig. 8. Failure loads.

was chosen to be $[\pm\theta]$. The displacements of carbon/epoxy pipes of three stacking sequences are shown in Fig. 9. It is shown that the deformation mode is dependent on the ply angle. When the ply angle is 0, all fibres are in the axial direction and the pipe can more easily deform in the hoop direction. Conversely, when the ply angle is 90°, the pipe shows concentrated deformation at the mid-span.

The failure loads vs. ply angle for the carbon/epoxy and glass/epoxy pipes are shown in Fig. 10. It is shown the failure load reaches the maximum when the ply angle is 75° for the carbon/epoxy composite and when the ply angle is 60° for the glass/epoxy composite. This is in agreement with the literature [21].

Table 3
Failure loads at various fibre volume fractions.

V_{fc}	V_{fg}	Failure load (N) $[0_C/90_G/45_C/-45_G]_S$	$[0_G/90_C/45_G/-45_C]_S$
30%	30%	3507	2904.2
30%	50%	3811.9	3714.4
50%	30%	4102.5	3737.9
50%	50%	4523.9	4142

3.2. Effect of fibre volume fraction

The effect of fibre volume fraction was studied for two stacking sequences $[0_C/90_G/45_C/-45_G]_S$ and $[0_G/90_C/45_G/-45_C]_S$. Two fibre volume fractions 30% and 50% were chosen for both the carbon/epoxy and glass/epoxy plies. The failure loads at various fibre volume fractions are shown in Table 3.

It is shown from Table 3 that the failure load increases with both fibre volume fractions and the hybrid composite has higher failure load when carbon/epoxy plies are placed at the outer surface.

3.3. Effect of hybridisation

When the ply angle was 0, 45° and 90°, respectively, glass/epoxy plies were substituted for some of the carbon/epoxy plies in the full carbon composite pipe. Two substitutions, i.e. from the outside and from the inside, were studied. The failure loads vs. the number of glass fibre plies are shown in Fig. 11. It is shown that when the ply angle is 0 and substitution occurs from the outside of the pipe, positive hybrid effects exist when less than half of the plies are glass/epoxy. Conversely, when substitution occurs from the inside of the pipe, positive hybrid effects exist when more than half of the plies are glass/epoxy. When the ply angle is 45°, the hybrid effects are mostly positive. When the ply angle is 90°, positive hybrid effects mostly occur when the substitution occurs from the inside of the pipe.

How hybridisation affects failure of the composite pipe was further studied by examining the failure sequence of all plies. When the ply angle is 45° and substitution is from the outside to the inside, the failure sequences of various hybrid composite pipes are shown in Table 4.

It is shown from Table 4 that failure is initiated at the outer surface for the full carbon fibre composite pipe. When the outermost ply is replaced by glass/epoxy, failure is initiated at the second outermost ply, i.e. at the carbon/epoxy ply. When there are 2–4 glass/epoxy plies on the outside of the hybrid composite pipe, failure is initiated at the inner surface. As more carbon/epoxy plies are replaced, failure initiation is back to the outer surface, immediately followed by the inner surface. For the full glass fibre composite pipe, failure is initiated at the inner surface. With reference to Fig. 11, the maximum failure is achieved when the outermost ply is replaced by glass/epoxy.

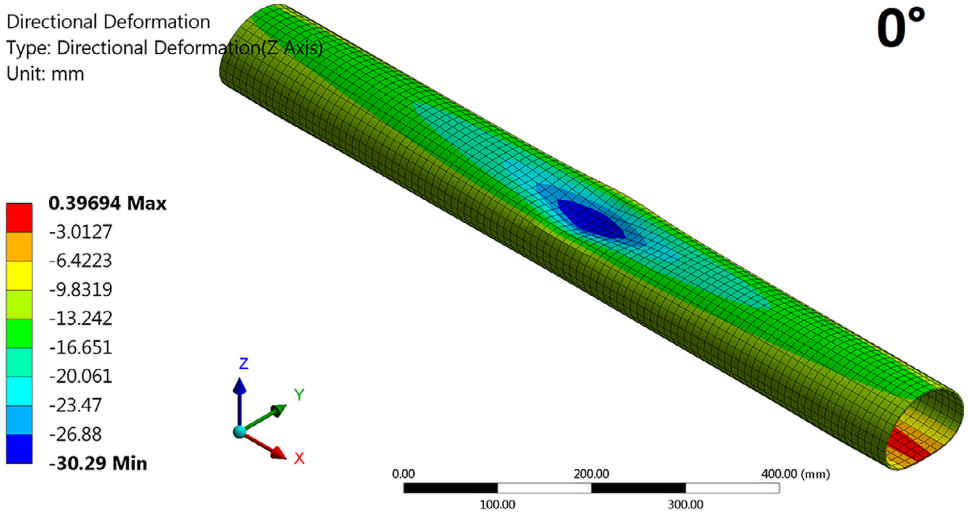

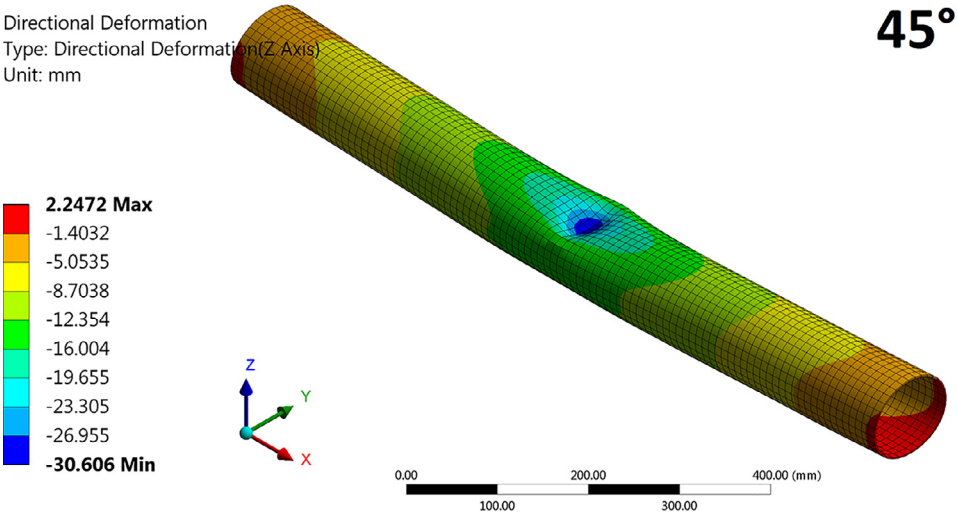

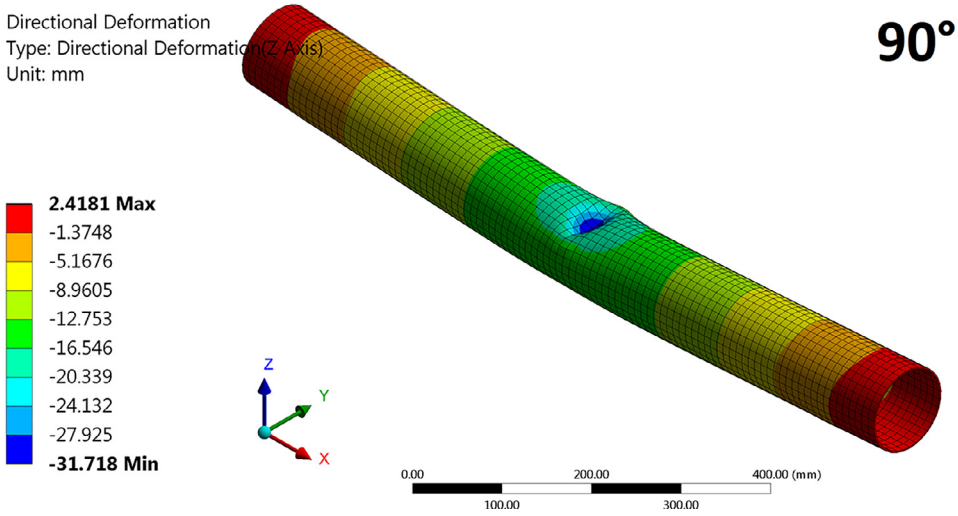

Fig. 9. The displacements of carbon/epoxy pipes.

Table 4
Failure sequences of various hybrid composite pipes when substitution is from the outside to the inside.

Number of glass/epoxy plies	Stacking sequence (outside to inside)	Ply failure sequence (first to last)							
0	$[\pm 45]_{2CS}$	1	2	3	8	4	7	6	5
1	$[45_G/-45_C/(\pm 45)_C/(\mp 45)_{2C}]$	2	8	1	3	4	7	6	5
2	$[(\pm 45)_G/(\pm 45)_C/(\mp 45)_{2C}]$	8	1	3	2	4	7	6	5
3	$[(\pm 45)_G/45_G/-45_C/(\mp 45)_{2C}]$	8	1	2	3	7	4	6	5
4	$[(\pm 45)_{2G}/(\mp 45)_{2C}]$	8	1	2	3	7	4	6	5
5	$[(\pm 45)_{2G}/-45_G/45_C/(\mp 45)_C]$	1	8	2	3	7	6	4	5
6	$[(\pm 45)_{2G}/(\mp 45)_G/(\mp 45)_C]$	1	8	3	2	7	4	6	5
7	$[(\pm 45)_{2G}/(\mp 45)_G/-45_G/45_C]$	1	8	7	3	2	6	4	5
8	$[\pm 45]_{2GS}$	8	7	1	6	2	3	4	5

Table 5
Failure sequences of various hybrid composite pipes when substitution is from the inside to the outside.

Number of glass/epoxy plies	Stacking sequence (outside to inside)	Ply failure sequence (first to last)							
0	$[\pm 45]_{2CS}$	1	2	3	8	4	7	6	5
1	$[(\pm 45)_{2C}/(\mp 45)_C/-45_C/45_G]$	8	1	2	3	4	7	6	5
2	$[(\pm 45)_{2C}/(\mp 45)_C/(\mp 45)_G]$	8	1	2	3	7	4	6	5
3	$[(\pm 45)_{2C}/-45_C/45_G/(\mp 45)_G]$	8	1	2	3	7	6	4	5
4	$[(\pm 45)_{2C}/(\mp 45)_{2G}]$	8	1	2	3	7	6	4	5
5	$[(\pm 45)_C/45_C/-45_G/(\mp 45)_{2G}]$	8	1	2	3	7	6	4	5
6	$[(\pm 45)_C/(\pm 45)_G/(\mp 45)_{2G}]$	8	1	2	7	3	6	4	5
7	$[45_C/-45_G/(\pm 45)_G/(\mp 45)_{2G}]$	1	8	7	3	2	6	4	5
8	$[\pm 45]_{2GS}$	8	7	1	6	2	3	4	5

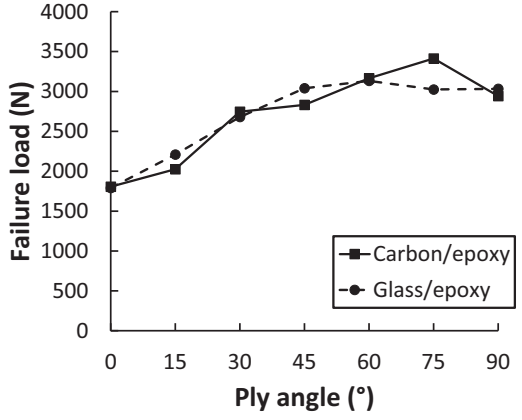

Fig. 10. Failure loads vs. ply angle for carbon/epoxy and glass/epoxy pipes.

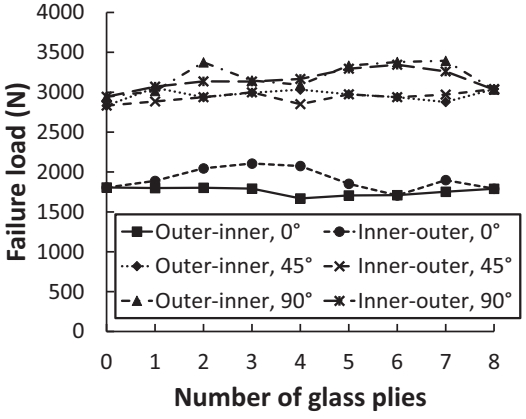

Fig. 11. Failure loads vs. number of glass plies.

When the ply angle is 45° and substitution is from the inside to the outside, the failure sequences of various hybrid composite pipes are shown in Table 5.

It is shown from Table 5 that when there are 1–6 glass/epoxy plies on the inside of the hybrid composite pipe, failure is initiated at the inner surface, immediately followed by the outer surface. When there are 7 glass/epoxy plies, failure is initiated at the outer surface, immediately followed by the inner surface.

4. Conclusions

The flexural behaviour of hybrid composite pipes reinforced with carbon and glass fibres was studied. The effects of ply angle, fibre volume fraction and hybridisation have been found. It is shown that the hybrid composite pipe can resist the maximum bending load when the ply angle is between 60° and 75° Failure load increases with the fibre volume fraction. The hybrid composite pipe has comparable failure loads compared to the full carbon fibre composite pipe or the full glass fibre composite pipe. This suggests that the cost and weight of composite pipes can be reduced via hybridisation. It is also shown that the location of failure initiation can be tailored by hybridising carbon and glass fibres. These conclusions point out a way to optimal design of fibre reinforced hybrid composite pipes.

Declaration of Competing Interest

There is no conflict of interest.

References

[1] M. Manoj Prabhakar, et al., An overview of burst, buckling, durability and corrosion analysis of lightweight FRP composite pipes and their applicability, Compos. Struct. 230 (2019) 111419.
[2] J.C. Hastie, M. Kashtalyan, I.A. Guz, Failure analysis of thermoplastic composite pipe (TCP) under combined pressure, tension and thermal gradient for an offshore riser application, Int. J. Press. Vessels Pip. 178 (2019) 103998.
[3] R. Rafiee, On the mechanical performance of glass-fibre-reinforced thermosetting-resin pipes: a review, Compos. Struct. 143 (2016) 151–164.

[4] M. Xia, H. Takayanagi, K. Kemmochi, Analysis of multi-layered filament-wound composite pipes under internal pressure, Compos. Struct. 53 (4) (2001) 483–491.
[5] M. Xia, K. Kemmochi, H. Takayanagi, Analysis of filament-wound fiber-reinforced sandwich pipe under combined internal pressure and thermomechanical loading, Compos. Struct. 51 (3) (2001) 273–283.
[6] J. Xing, P. Geng, T. Yang, Stress and deformation of multiple winding angle hybrid filament-wound thick cylinder under axial loading and internal and external pressure, Compos. Struct. 131 (2015) 868–877.
[7] J. Bai, P. Seeleuthner, P. Bompard, Mechanical behaviour of ± 55 ° filament-wound glass-fibre/epoxy-resin tubes: I. Microstructural analyses, mechanical behaviour and damage mechanisms of composite tubes under pure tensile loading, pure internal pressure, and combined loading, Compos. Sci. Technol. 57 (2) (1997) 141–153.
[8] M. Xia, H. Takayanagi, K. Kemmochi, Analysis of transverse loading for laminated cylindrical pipes, Compos. Struct. 53 (3) (2001) 279–285.
[9] M. Xia, H. Takayanagi, K. Kemmochi, Bending behavior of filament-wound fiber-reinforced sandwich pipes, Compos. Struct. 56 (2) (2002) 201–210.
[10] A.K. Jonnalagadda, et al., An analytical model for composite tubes with bend–twist coupling, Compos. Struct. 131 (2015) 578–584.
[11] M. Stefanovska, et al., Theoretical and experimental bending properties of composite pipes, Int. J. Environ. Ecol. Eng. 102 (2015) 706–710.
[12] G. Marom, et al., Hybrid effects in composites: conditions for positive or negative effects versus rule-of-mixtures behaviour, J. Mater. Sci. 13 (7) (1978) 1419–1426.
[13] C. Dong, H.A. Ranaweera-Jayawardena, I.J. Davies, Flexural properties of hybrid composites reinforced by S-2 glass and T700S carbon fibres, Compos. Part B: Eng. 43 (2) (2012) 573–581.
[14] C. Dong, J. Duong, I.J. Davies, Flexural properties of S-2 glass and TR30S carbon fiber-reinforced epoxy hybrid composites, Polym Compos 33 (5) (2012) 773–781.
[15] C. Dong, I.J. Davies, Flexural properties of glass and carbon fiber reinforced epoxy hybrid composites, Proc. Inst. Mech. Eng. Part L: J. Mater. Des. Appl. 227 (4) (2013) 308–317.
[16] C. Dong, Sudarisman, I.J. Davies, Flexural properties of E glass and TR50S carbon fiber reinforced epoxy hybrid composites, J. Mater. Eng. Perform. 22 (1) (2013) 41–49.
[17] P.W. Manders, M.G. Bader, The strength of hybrid glass/carbon fibre composites, J. Mater. Sci. 16 (8) (1981) 2233–2245.
[18] M.R. Garnich, V.M.K. Akula, Review of degradation models for progressive failure analysis of fiber reinforced polymer composites, Appl. Mech. Rev. 62 (1) (2009) 010801-1–010801-33.
[19] B. Bilyeu, W. Brostow, K.P. Menard, Epoxy thermosets and their applications I: chemical structures and applications, J. Mater. Educ. 21 (5/6) (1999) 281–286.
[20] T.-.W. Chou, Microstructural Design of Fiber Composites, Cambridge University Press, Cambridge, U.K., 1992.
[21] G. Meijer, F. Ellyin, A failure envelope for ±60° filament wound glass fibre reinforced epoxy tubulars, Compos. Part A 39 (3) (2008) 555–564.